Ultrafast Exciton Energy Transfer between Nanoscale Coaxial Cylinders: Intertube Transfer and Luminescence Quenching in Double-Walled Carbon Nanotubes

Takeshi Koyama,[†,*] Yuki Asada,[‡] Naoki Hikosaka,[†] Yasumitsu Miyata,[‡] Hisanori Shinohara,[‡] and Arao Nakamura[†]

[†]Department of Applied Physics, Graduate School of Engineering, Nagoya University, Chikusa, Nagoya 464-8603, Japan, and [‡]Department of Chemistry, Graduate School of Science, Nagoya University, Chikusa, Nagoya 464-8602, Japan

ABSTRACT We study exciton energy transfer in double-walled carbon nanotubes using femtosecond time-resolved luminescence measurements. From direct correspondence between decay of the innertube luminescence and the rise behavior in outertube luminescence, it is found that the time constant of exciton energy transfer from the inner to the outer semiconducting tubes is ~150 fs. This ultrafast transfer indicates that the relative intensity of steady-state luminescence from the innertubes is ~700 times weaker than that from single-walled carbon nanotubes.

KEYWORDS: double-walled carbon nanotubes · exciton energy transfer · one-dimensional exciton · photoluminescence · femtosecond time-resolved luminescence spectroscopy

Double-walled carbon nanotubes (DWNTs) are coaxial hollow cylinders of graphene sheets with diameters in the range of ~1 nm, lengths of ~1 μm, and intertube (wall-to-wall) distances of ~0.32–0.42 nm.[1] DWNTs have attracted significant attention for applications utilizing their favorable properties, such as high thermal and electronic conductivities, as well as fundamental interest, from physics and chemistry viewpoints, in the thermal, electronic, and optical properties as a consequence of their unique structure. Since the geometrical structure of carbon atoms determines either semiconducting or metallic properties of a nanotube, DWNTs have four configurations; both inner- and outertubes are semiconducting or metallic, either inner- or outertube is semiconducting and the other is metallic. One of the current issues in their optical properties is photoluminescence from the inner semiconducting tubes. Strong photoluminescence comparable to that from single-walled carbon nanotubes (SWNTs) has been observed in the spectral range of the innertubes.[2−10] However, Okazaki *et al.* and other groups have reported that the photoluminescence from the innertubes is quenched,[11−14] implying exciton energy transfer to the outertubes. The reason for these different results was explained by the difference in the amount of luminescent impurities, that is, SWNTs, in the DWNT sample.[12,13] Nevertheless, the occurrence of innertube luminescence in DWNTs is still under debate.

Exciton energy transfer between carbon nanotubes is of major interest[15−26] because the distance between donor and acceptor tubes is equivalent to or shorter than the size of quasi-one-dimensional excitons. In such a case, the well-known Förster model based on the point dipole approximation breaks down; examples include light-harvesting complexes[27−30] and conjugated polymers,[31,32] as well as carbon nanotubes.[21,24−26,33,34] The exciton size in carbon nanotubes is estimated to be ~1−2 nm,[35−38] which is equivalent to the intertube distances between SWNTs packed in bundles. A theoretical calculation within a distributed transition monopole approximation has shown that the transfer rate of excitons between two 10 nm long semiconducting SWNTs with a separation of 1.4 nm (intertube distance ~0.6 nm) is 9.7×10^{12} s^{-1}, which is about 3 orders of magnitude smaller than the value of 4.0×10^{15} s^{-1} obtained by the point dipole approximation calculation.[21] Experimental studies have recently confirmed this situation. The transfer rate between a DNA-wrapped SWNT pair at an intertube distance of ~0.9 nm measured by near-field microscopy is $(0.3–5.0) \times 10^{12}$ s^{-1}.[19] Our time-resolved luminescence measurements

* Address correspondence to koyama@nuap.nagoya-u.ac.jp.

Received for review May 6, 2011 and accepted June 11, 2011.

Published online June 17, 2011
10.1021/nn201661q

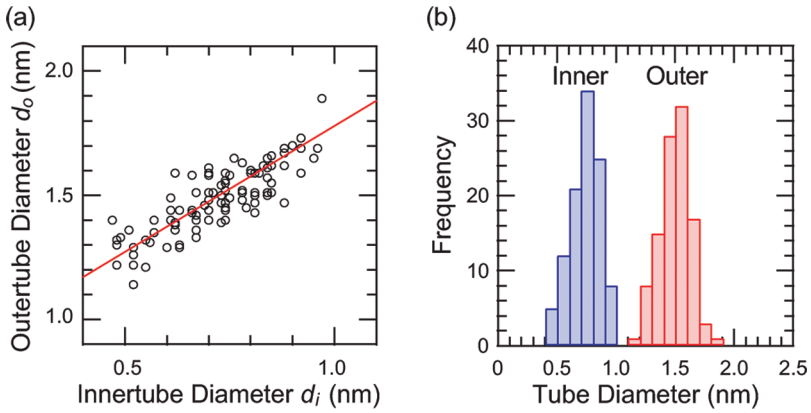

Figure 1. (a) Relationship between the innertube diameter, d_i, and the outertube diameter, d_o. The straight line is d_o (nm) = 0.76 + 1.02d_i. (b) Histogram of the diameter distributions of the inner- and outertubes.

showed a transfer rate of 2.7×10^{11} s^{-1} at an intertube distance of ~0.9 nm in polyfluorene-wrapped SWNT bundles[25] and a rate of $(1.8-1.9) \times 10^{12}$ s^{-1} at an intertube distance of ~0.34 nm in bare SWNT bundles.[26]

In DWNTs, exciton energy transfer from the inner semiconducting tube to the outer semiconducting or metallic tube is expected to occur: If the outertube is semiconducting, it has a narrower band gap than the inner semiconducting tube due to its larger diameter. On the other hand, if the outertube is metallic, there are continuous states over the innertube gap. Exciton energy transfer in DWNTs shows some unique features: (i) The transfer takes place between coaxial cylinders on the nanoscale, and (ii) the intertube distance is almost constant through the length of the tube and is easy to determine. Transient absorption measurements[39] have indicated that excitons transfer from the inner- to the outertubes in ~0.4 ps; such fast transfer implies strong quenching of innertube luminescence. In contrast, time-resolved luminescence measurements[2,7] and a recent transient absorption study[40] have suggested that the innertube exciton decays within several tens of picoseconds, and such a long decay time implies considerable innertube luminescence. Thus, the dynamics of exciton energy transfer in DWNTs remain controversial.

One possible crucial problem in these time-resolved measurements in DWNTs as well as the steady-state measurements is the quality of the samples used in these previous studies, wherein SWNTs are contained as impurities in the DWNT samples, as pointed out in refs 12,13, and 41. To obtain isolated DWNTs for optical measurements, a micellization process is often carried out that uses vigorous sonication. In ref 41, Miyata *et al.* have shown that the abundance of SWNTs with respect to DWNTs drastically increased from less than ~5 to 50% after sonication. This is because the innertubes are extracted during the micellization process. Consequently, it is very possible that these SWNT impurities affect the optical response after the micellization process. However, little attention has been paid to this point in prior studies.

In this paper, we investigate exciton dynamics in DWNTs to elucidate the issue of innertube luminescence by using time-resolved luminescence measurements on (i) a DWNT film sample not subjected to a micellization process, (ii) an unpurified DWNT solution sample subjected to only a micellization process, and (iii) a purified DWNT solution sample subjected to a micellization process as well as further density gradient ultracentrifugation (DGU). Exciton energy transfer from the inner- to the outertubes was found to take place in the femtosecond regime, indicating quenching of innertube luminescence. This study demonstrates the unique energy transfer of one-dimensional excitons between coaxial cylinders on a nanometer scale.

The DWNTs investigated in this study were synthesized by an alcohol catalytic chemical vapor deposition process and purified by thermal oxidation. These synthesized nanotubes were used to form film samples (consisting of bundled DWNTs) and were also used as starting materials for further processing for other DWNT samples. The relative abundance of DWNTs with respect to SWNTs and triple-walled carbon nanotubes (TWNTs) in the film samples was measured by transmission electron microscopy (TEM). The typical abundance of the DWNTs was 87%, compared to 1% for SWNTs and 12% for TWNTs, ensuring that luminescence observed in the film samples is predominantly from the DWNTs. From TEM observations, we also determined the relationship between the innertube diameter d_i and the outertube diameter d_o, as plotted in Figure 1a. The data could be fitted to a straight line d_o (nm) = 0.76 + 1.02d_i; d_o thus shows a linear dependence on d_i. The mean intertube distance of 0.38 (=0.76/2) nm is in the range of previously reported values of ~0.32−0.42 nm.[1] Diameter distributions of inner- and outertubes are displayed in Figure 1b. The distributions of the innertube (~0.4−1.0 nm) and outertube (~1.2−1.8 nm) diameters indicate no overlap between the two.

A solution sample was prepared and subjected only to a micellization process reported in ref 42. This was

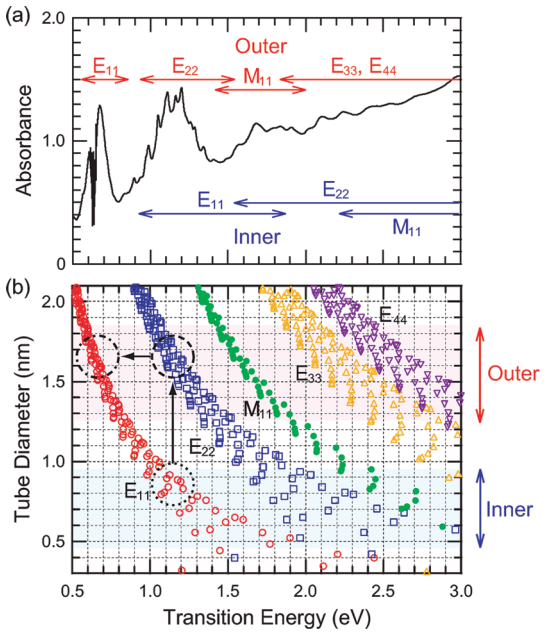

Figure 2. (a) Absorption spectrum of an unpurified solution sample. (b) Kataura plot for the E_{11}, E_{22}, M_{11}, E_{33}, and E_{44} transitions.

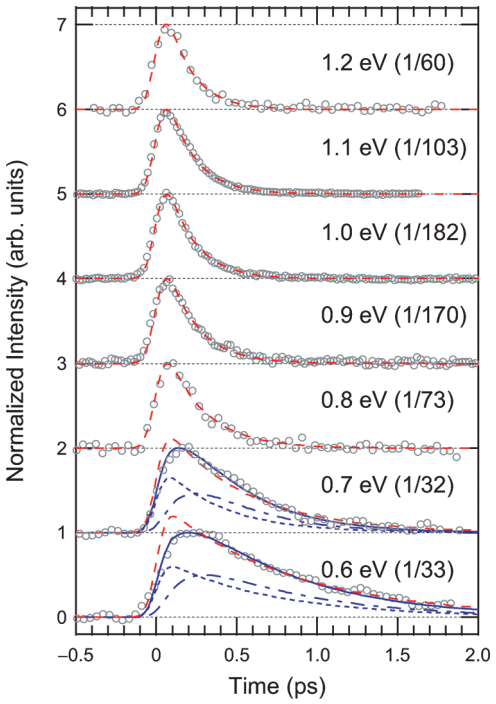

Figure 3. Luminescence kinetics at 0.6−1.2 eV in the film sample. For clarity of viewing, the decay curves are normalized at the maxima (normalization factors are indicated in parentheses) and the baselines are shifted. The circles, red dashed, and blue solid lines represent the results of the experiment, single exponential fitting, and exponential fitting involving a rise component, respectively. The blue chain and dotted lines represent the components with and without the rise term.

used as the unpurified solution sample. Another solution sample was prepared by a micellization process and further DGU by using the method described in ref 41. Thus, in this case, the SWNTs extracted during the micellization process were removed, and this solution was used as a purified solution sample.

Figure 2a shows the absorption spectrum of the unpurified solution sample. We examined spectral overlap between the inner- and outertubes by considering the relationship between the tube diameter and transition energy, the so-called Kataura plot, in Figure 2b. The E_{11} and E_{22} energies were calculated using the expressions given by eq 1a,b in ref 43 for isolated SWNTs in sodium dodecyl sulfate micelles. The M_{11} (the first exciton transition in metallic nanotubes), E_{33}, and E_{44} energies are plotted using the expressions given by eq 1 in ref 44 for isolated SWNTs in air. Here, E_{ii} (M_{ii}) (i = 1,2,...) indicates exciton transition associated with the ith valence and conduction bands in a semiconducting (metallic) nanotube. These five transition energies may be shifted in our samples compared to the data in the previous studies because the environment around the nanotubes is different; that is, the surfactant in the present study is sodium cholate, not sodium dodecyl sulfate;[2] the nanotubes are in a solvent, not in air,[45,46] and the innertubes are surrounded by the outertubes.[6] However, the shifts are several tens of millielectronvolts, comparable to the spectral resolution of ~0.03 eV in our luminescence measurements. The absorption structure observed below 0.8 eV is attributed only to the E_{11} bands in the outertubes (the dips in the 0.50−0.55 eV range are due to absorption by deuterium oxide). In the range of 0.9−1.5 eV, the E_{22} bands in the outertubes overlap with the inner E_{11} bands. Above 1.5 eV, the M_{11}, E_{33}, and E_{44} bands in the outertubes and the E_{11}, E_{22}, and M_{11} bands in the innertubes overlap with each other. In this study, special attention was paid to the spectral separation of the inner and outer E_{11} bands and the overlap between the inner E_{11} and the outer E_{22} bands.

TABLE 1. Values of the Parameters for Exponential Fitting and Rate-Equation Analysis for the Film Sample[a]

decay kinetics (eV)	I	τ (fs)	I_i	I_o	$\gamma_i^{t^{-1}}$ (fs)	$\gamma_o^{t^{-1}}$ (fs)
1.2	60	160				
1.1	100	170				
0.7			16	16	150	380
0.6			17	16	150	670

[a] I and τ are the initial intensity and the decay time constant at 1.1 and 1.2 eV (innertubes). I_i and I_o are the initial intensities of the components with and without the rise terms at 0.6 and 0.7 eV (outertubes), respectively. $\gamma_i^{t^{-1}}$ and $\gamma_o^{t^{-1}}$ are the rise and decay time constants at 0.6 and 0.7 eV (outertubes), respectively.

Luminescence kinetics in the 0.6−1.2 eV range in the film sample are shown in Figure 3. For clarity in displaying the decay behavior, the ordinate represents the normalized intensity and baselines are shifted. As shown in the absorption spectrum in Figure 2a, luminescence at 0.6 and 0.7 eV is due to the outertubes, and that at 0.8−1.2 eV is due to the innertubes.

We performed curve-fitting analysis with a single exponential function $I\ \exp(-t/\tau)$ convoluted with the instrument response function. The single exponential function represents simple exciton decay with a time constant τ. The fitted results are plotted as red dashed lines in Figure 3, and the fitted parameters for the decay kinetics at 1.1 and 1.2 eV are listed in Table 1. Since the obtained time constants (160 and 170 fs) are larger than the decay time of E_{22} excitons (40−60 fs),[47,48] the luminescence observed at these energies is not due to the E_{22} excitons in the outertubes and is assigned to the E_{11} luminescence from the innertubes. At 0.8−1.2 eV (innertube luminescence), the fitted curves reproduce the experimental data well. In contrast, the experimental results at 0.6 and 0.7 eV (outertube luminescence) cannot be fitted to the above function around the time origin. This disagreement indicates that the experimental curves have a rise term. Since our similar luminescence experiments on bundled SWNTs showed no apparent rise behavior at 0.6 and 0.7 eV,[26] the rise term observed here arises from neither intratube exciton relaxation nor a bundling effect. Therefore, the observed behavior suggests exciton energy transfer from the inner- to the outertubes.

In the Förster−Dexter formalism[49,50] describing excitation energy transfer due to electron exchange and interactions between transition moments, the exciton transfer rate depends on the spectral overlap and the donor−acceptor distance. Since the intertube distances in the DWNTs are in the range of ∼0.32−0.42 nm,[1] the inner E_{11} bands overlap with the E_{22} bands in the corresponding outertubes, as shown in Figure 2b. Thus, an exciton of the E_{11} band in an innertube transfers effectively to the E_{22} band in the corresponding outertube, which is nearest to the innertube. We consider an example where the E_{11} energies of the innertubes are 1.1−1.2 eV. The Kataura plot in Figure 2b indicates that the diameters of these innertubes are in the range of 0.8−0.9 nm (indicated by the dotted circle). Taking the mean intertube difference in the DWNTs in this study to be ∼0.38 nm (*i.e.*, diameter difference of ∼0.76 nm), we find that the diameters of the corresponding outertubes are 1.6−1.7 nm (see the upward arrow). These outertubes have E_{22} energies of 1.0−1.2 eV (dashed circle), which spectrally overlaps with the inner E_{11} energy. The outertubes with the E_{22} energies of 1.0−1.2 eV have E_{11} energies of 0.6−0.7 eV (chain circle). Consequently, the signature of the exciton energy transfer observed in the 0.6−0.7 eV luminescence should correspond to the decay behavior in the 1.1−1.2 eV luminescence.

To analyze the dynamical behavior of photoluminescence from the inner- and outertubes, we consider exciton relaxation processes in bundled DWNTs, schematically shown in Figure 4. The pulse excitation at 1.55 eV creates excitons in both the inner E_{11} band and the

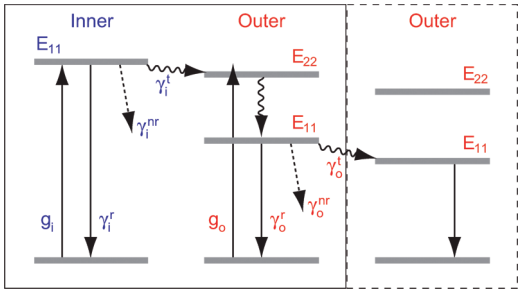

Figure 4. Diagram of exciton relaxation processes in bundled DWNTs.

outer E_{22} band with generation functions g_i and g_o, respectively. Excitons in the inner E_{11} band decay due to internal processes, *i.e.*, radiative and nonradiative decay with rates of γ_i^r and γ_i^{nr}, and a competitive external process, *i.e.*, energy transfer to the outer E_{22} band with the rate γ_i^t. Since excitons in the outer E_{22} band quickly relax to the outer E_{11} band within several tens of femtoseconds,[47,48] this relaxation term can be neglected compared to the time resolution of our experiments. Like the excitons in the inner E_{11} band, those in the outer E_{11} band decay by radiative and nonradiative processes with rates γ_o^r and γ_o^{nr}, respectively. Owing to the bundled structure, they also experience energy transfer to adjacent narrower gap DWNTs with the rate γ_o^t. The rate equations for exciton densities n_i and n_o are written in the form

$$\begin{cases} \dfrac{dn_i(t)}{dt} = g_i - (\gamma_i^r + \gamma_i^{nr} + \gamma_i^t)n_i(t) \\ \dfrac{dn_o(t)}{dt} = g_o + \gamma_i^t n_i(t) - (\gamma_o^r + \gamma_o^{nr} + \gamma_o^t)n_o(t) \end{cases} \quad (1)$$

For the dynamics after the pulse excitation, the solution of eq 1 is given by

$$\begin{cases} n_i(t) = N_i \exp[-(\gamma_i^r + \gamma_i^{nr} + \gamma_i^t)t] \\ n_o(t) = N_o \exp[-(\gamma_o^r + \gamma_o^{nr} + \gamma_o^t)t] \\ \qquad + \dfrac{N_i}{1 - (\gamma_o^r + \gamma_o^{nr} + \gamma_o^t)/(\gamma_i^r + \gamma_i^{nr} + \gamma_i^t)} \\ \qquad \times \{\exp[-(\gamma_o^r + \gamma_o^{nr} + \gamma_o^t)t] \\ \qquad\quad - \exp[-(\gamma_i^r + \gamma_i^{nr} + \gamma_i^t)t]\} \end{cases} \quad (2)$$

where N_i and N_o are the initial exciton densities for the inner- and outertubes created by the laser pulse. In the expression for $n_o(t)$, the first term represents a decay of excitons initially created in the outertube by the pulse excitation, and the second term gives kinetics of excitons transferred from the innertube. Since the luminescence intensity is proportional to the exciton density, the luminescence kinetics are expressed by eq 2.

Time-resolved luminescence measurements of isolated SWNTs[2,51,52] showed that the time constant of exciton decay (*i.e.*, the inverse of the sum of the radiative γ_{SWNT}^r and nonradiative γ_{SWNT}^{nr} decay rates, is on the order of 10−100 ps. The radiative decay rate at a specific transition energy is a function of the oscillator strength, electron mass, and refractive index. The

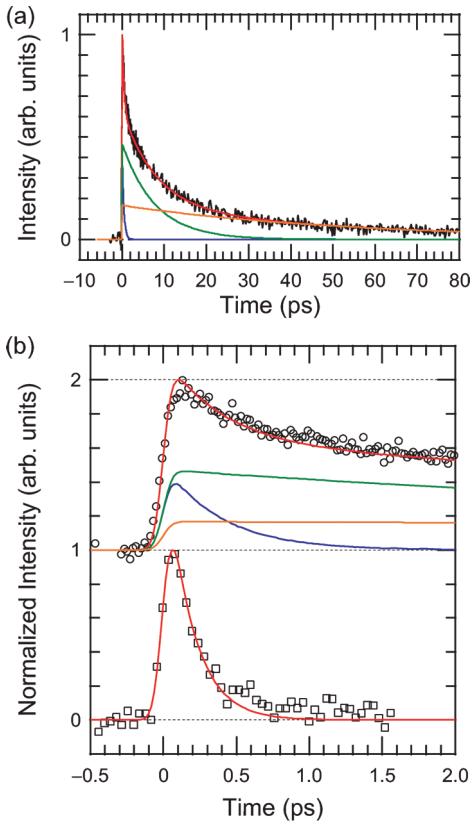

Figure 5. (a) Luminescence kinetics at 1.1 eV in an unpurified solution sample. The colored lines are the results of the fitting calculations. Blue, green, and orange lines represent the fast, medium, and slow components, respectively. The red line represents the sum of the three components. (b) Luminescence kinetics in a short time scale at 1.1 eV in unpurified (top) and purified (bottom) solution samples. For clarity of viewing, the decay curves are normalized and the baselines are shifted. The symbols and colored lines represent the results of experiment and exponential fitting.

nonradiative decay rate is dependent on the positions of the energy levels of dark states relative to the bright state, the densities of defects and impurities on the tube surface, and the probability of multiphonon emission processes. Since the values of these parameters likely have the same order of magnitude as those for the isolated SWNTs, we substitute $\gamma^{r}_{SWNT} + \gamma^{nr}_{SWNT} = (10-100\ ps)^{-1}$ into $(\gamma^{r}_{j} + \gamma^{nr}_{j})$ (j = i, o) in eq 2. Using the expression for $n_o(t)$, the decay curves at 0.6 and 0.7 eV are fitted and the results are plotted, shown by the solid blue lines in Figure 3; the first and second terms in $n_o(t)$ are plotted by blue dotted and chain lines in the figure, respectively. The fitted parameters are listed in Table 1. The rise time $\gamma_i^{t^{-1}}$ (=150 fs) of the outertube luminescence corresponds well to the decay time τ (=160−170 fs) of the innertube luminescence. This correspondence indicates that the exciton energy transfer from the innertube to the outertube occurs with this time constant. Since we used the DWNT ensemble sample with different chiralities, the obtained time constant of exciton energy transfer is a weighted average for the ensemble. The transfer rate

TABLE 2. Values of Parameters of Fitting Calculations for 1.1 eV Luminescence in the Unpurified Solution Sample[a]

I_1	I_2	I_3	τ_1 (ps)	τ_2 (ps)	τ_3 (ps)
0.44	0.41	0.15	0.39	7.80	54.10

[a] I_1, I_2, and I_3 (=1 − I_1 − I_2) are the initial intensities; τ_1, τ_2, and τ_3 are the time constants.

of ∼6.6 × 10^{12} s^{-1} [∼(150 × 10^{-15}s)$^{-1}$] is larger than the rate of (1.8−1.9) × 10^{12} s^{-1} between adjacent SWNTs with an intertube distance of ∼0.34 nm (center-to-center distance of ∼1.34 nm) in bundles.[26] The larger transfer rate in the DWNTs is reasonable because the donor is cylindrically surrounded by the acceptor.

We next investigate luminescence kinetics of the unpurified and purified solution samples to compare the decay behaviors of the various samples prepared by different processes. Figure 5a shows the decay curve at 1.1 eV in the unpurified solution sample. This decay behavior is much slower than that of the film sample shown in Figure 3. The decay curve is fitted to a triple exponential function $I_1\exp(-t/\tau_1) + I_2\exp(-t/\tau_2) + I_3\exp(-t/\tau_3)$ convoluted with the instrument response function. The fitted results, total and respective components, are plotted using different colored lines in Figure 5a, and the values of the fitted parameters are listed in Table 2. The decay time constants are τ_1 = 0.39 ps, τ_2 = 7.80 ps, and τ_3 = 54.10 ps. These values are consistent with the decay times widely observed in semiconducting SWNTs dispersed in aqueous surfactants.[2,51,53] The luminescence kinetics in a short time scale are replotted at the top in Figure 5b, and the bottom shows the kinetics at 1.1 eV in the purified solution sample wherein the SWNTs are removed by DGU. The decay curve for the purified solution sample is fitted to a single exponential function with a time constant of 170 fs, which is in good agreement with the results of the film sample. In contrast, the long-lived luminescence observed in the unpurified solution sample indicates that this sample contains SWNTs with smaller diameters corresponding to the E_{11} energies of the innertubes in DWNTs. These results indicate that the unpurified solution sample contains SWNTs that are the innertubes of the DWNTs extracted during the micellization process, as pointed out in ref 41, in addition to the residual SWNTs in the starting materials of the DWNTs.

Finally, we estimate the quantum efficiency η_i of the innertube luminescence relative to the efficiency η_{SWNT} of the isolated SWNT luminescence. Since the quantum efficiency of luminescence is generally defined as $\gamma^r/(\gamma^r + \gamma^{nr})$ with the radiative decay rate γ^r and the total nonradiative decay rate γ^{nr}, the ratio η_i/η_{SWNT} is given by $(\gamma_i^r/\gamma_{SWNT}^r) \times (\gamma_{SWNT}^r + \gamma_{SWNT}^{nr})/(\gamma_i^r + \gamma_i^{nr} + \gamma_i^t)$. As explained above, γ_i^r and γ_i^{nr} should have values similar to those of γ_{SWNT}^r and γ_{SWNT}^{nr}, respectively. Hence, η_i/η_{SWNT} is transformed into $\sim[1 + \gamma_i^t/(\gamma_{SWNT}^r + \gamma_{SWNT}^{nr})]^{-1}$. Using the typical value of $\gamma_{SWNT}^r + \gamma_{SWNT}^{nr} \sim (100\ ps)^{-1}$ and

$\gamma_i^t \sim (150\ \text{fs})^{-1}$, η_i/η_{SWNT} is calculated to be ~1/700. This low efficiency indicates strong quenching of innertube luminescence due to the ultrafast exciton energy transfer. Therefore, we can understand that the discrepancy between the results in the present work and those in the literature which reported the apparent innertube luminescence in aqueous suspended DWNTs, arises from the residual SWNTs present in the starting materials[12,13] and the extracted SWNTs from DWNTs.[41]

In summary, we carried out femtosecond time-resolved luminescence measurements on double-walled carbon nanotubes and demonstrated ultrafast exciton energy transfer between the inner- and outertubes of the double-walled carbon nanotube ensemble with a time constant of ~150 fs. It is found that the relative intensity of steady-state luminescence from the innertubes is ~700 times weaker than that from single-walled carbon nanotubes. This work clearly demonstrates a rate of exciton energy transfer in double-walled carbon nanotubes that is equivalent to ideal coaxial cylinders with an average intertube distance of ~0.38 nm. The exciton energy transfer rate is a key parameter to understand the transfer mechanism in this unique geometric structure.

EXPERIMENTAL METHODS

The DWNTs were synthesized by an alcohol catalytic chemical vapor deposition process. Thermal oxidation (700 °C, 30 min) was carried out to purify DWNTs against SWNTs. These synthesized nanotubes were used to form film samples (consisting of bundled DWNTs) and were also used as starting materials for further processing for other DWNT samples. A solution sample was prepared and subjected only to a micellization process. The DWNTs (1.5 mg) were dispersed in deuterium oxide (5.5 g) with 1.5 wt % surfactant (sodium cholate) by sonication at 10 W for 2 h. The dispersion was then immediately centrifuged at 120 000*g* for 1.5 h, and the upper 80% supernatant was collected. This supernatant was used as the unpurified solution sample. Another solution sample was prepared by a micellization process and further DGU by using the method described in ref 41. This solution was used as a purified solution sample.

High-resolution transmission electron microscope (HRTEM) observations were carried out on a JEM-2100F (JEOL) high-resolution field-emission gun TEM operated at 80 kV at room temperature and under a pressure of 10^{-6} Pa. HRTEM images were recorded with a charge-coupled device with an exposure time of typically 1 s.

Time-resolved luminescence measurements were performed by employing the frequency up-conversion technique.[25,26] The light source was a mode-locked Ti:sapphire laser with a repetition rate of 82 MHz, wavelength of 800 nm (photon energy 1.55 eV), and a pulse width of 80 fs. The excitation photon energy of 1.55 eV is situated in the high energy tails of the E_{11} bands of the innertubes as well as the E_{22} bands of the outertubes. The excitation intensity is ~1 μJ/cm^2 per pulse, which is below the threshold (~30−50 μJ/cm^2 per pulse) of nonlinear processes of exciton decay.[54,55] The instrument response function of the measurement system was determined by measuring the cross-correlation trace between the gate pulse and excitation pulse scattered from the sample surface, which had a Gaussian shape with a full width at half-maximum of 120 fs. The spectral resolution was about 0.03 eV.

Acknowledgment. The authors would like to thank Dr. M. Yoshikawa and Mr. K. Sato (Toray Industries, Inc.) for preparation of the DWNTs. This work has been supported by a Grant-in-Aid for Scientific Research on Priority Areas "Carbon Nanotube Nanoelectronics" from the Ministry of Education, Culture, Sports, Science and Technology of Japan.

Note Added after ASAP Publication: After this paper was published ASAP June 17, 2011, corrections were made to eq 2. The revised version was published June 21, 2011.

REFERENCES AND NOTES

1. Pfeiffer, R.; Pichler, T.; Kim, Y. A.; Kuzmany, H. Double-Wall Carbon Nanotubes. In *Carbon Nanotubes: Advanced Topics in Synthesis, Properties, and Applications, Topics in Applied Physics*; Jorio, A., Dresselhaus, M. S., Dresselhaus, G., Eds.; Springer: Berlin, 2008; Vol. 111, pp 495−530.
2. Hertel, T.; Hagen, A.; Talalaev, V.; Arnold, K.; Hennrich, F.; Kappes, M.; Rosenthal, S.; McBride, J.; Ulbricht, H.; Flahaut, E. Spectroscopy of Single- and Double-Walled Carbon Nanotubes in Different Environments. *Nano Lett.* **2005**, *5*, 511–514.
3. Iakoubovskii, K.; Minami, N.; Kazaoui, S.; Ueno, T.; Miyata, Y.; Yanagi, K.; Kataura, H.; Ohshima, S.; Saito, T. IR-Extended Photoluminescence Mapping of Single-Wall and Double-Wall Carbon Nanotubes. *J. Phys. Chem. B* **2006**, *110*, 17420–17424.
4. Kishi, N.; Kikuchi, S.; Ramesh, P.; Sugai, T.; Watanabe, Y.; Shinohara, H. Enhanced Photoluminescence from Very Thin Double-Wall Carbon Nanotubes Synthesized by the Zeolite-CCVD Method. *J. Phys. Chem. B* **2006**, *110*, 24816–24821.
5. Hayashi, T.; Shimamoto, D.; Kim, Y. A.; Muramatsu, H.; Okino, F.; Touhara, H.; Shimada, T.; Miyauchi, Y.; Maruyama, S.; Terrones, M.; *et al.* Selective Optical Property Modification of Double-Walled Carbon Nanotubes by Fluorination. *ACS Nano* **2008**, *2*, 485–488.
6. Iakoubovskii, K.; Minami, N.; Ueno, T.; Kazaoui, S.; Kataura, H. Optical Characterization of Double-Wall Carbon Nanotubes: Evidence for Inner Tube Shielding. *J. Phys. Chem. C* **2008**, *112*, 11194–11198.
7. Hirori, H.; Matsuda, K.; Kanemitsu, Y. Exciton Energy Transfer between the Inner and Outer Tubes in Double-Walled Carbon Nanotubes. *Phys. Rev. B* **2008**, *78*, 113409/1−4.
8. Kim, J. H.; Kataoka, M.; Kim, Y. A.; Shimamoto, D.; Muramatsu, H.; Hayashi, T.; Endo, M.; Terrones, M.; Dresselhaus, M. S. Diameter-Selective Separation of Double-Walled Carbon Nanotubes. *Appl. Phys. Lett.* **2008**, *93*, 223107/1−3.
9. Shimamoto, D.; Muramatsu, H.; Hayashi, T.; Kim, Y. A.; Endo, M.; Park, J. S.; Saito, R.; Terrones, M.; Dresselhaus, M. S. Strong and Stable Photoluminescence from the Semiconducting Inner Tubes within Double Walled Carbon Nanotubes. *Appl. Phys. Lett.* **2009**, *94*, 083106/1−3.
10. Kim, J. H.; Kataoka, M.; Shimamoto, D.; Muramatsu, H.; Jung, Y. C.; Hayashi, T.; Kim, Y. A.; Endo, M.; Park, J. S.; Saito, R.; *et al.* Raman and Fluorescence Spectroscopic Studies of a DNA-Dispersed Double-Walled Carbon Nanotube Solution. *ACS Nano* **2010**, *4*, 1060–1066.
11. Okazaki, T.; Bandow, S.; Tamura, G.; Fujita, Y.; Iakoubovskii, K.; Kazaoui, S.; Minami, N.; Saito, T.; Suenaga, K.; Iijima, S. Photoluminescence Quenching in Peapod-Derived Double-Walled Carbon Nanotubes. *Phys. Rev. B* **2006**, *74*, 153404/1−4.
12. Green, A. A.; Hersam, M. C. Processing and Properties of Highly Enriched Double-Wall Carbon Nanotubes. *Nat. Nanotechnol.* **2009**, *4*, 64–70.
13. Tsyboulski, D. A.; Hou, Y.; Fakhri, N.; Ghosh, S.; Zhang, R.; Bachilo, S. M.; Pasquali, M.; Chen, L.; Liu, J.; Weisman, R. B. Do Inner Shells of Double-Walled Carbon Nanotubes Fluoresce? *Nano Lett* **2009**, *9*, 3282–3289.

14. Green, A. A.; Hersam, M. C. Properties and Application of Double-Walled Carbon Nanotubes Sorted by Outer-Wall Electronic Type. *ACS Nano* **2011**, *5*, 1459–1467.
15. Torrens, O. N.; Milkie, D. E.; Zheng, M.; Kikkawa, J. M. Photoluminescence from Intertube Carrier Migration in Single-Walled Carbon Nanotube Bundles. *Nano Lett.* **2006**, *6*, 2864–2867.
16. Berger, S.; Voisin, C.; Cassabois, G.; Delalande, C.; Roussignol, P.; Marie, X. Temperature Dependence of Exciton Recombination in Semiconducting Single-Wall Carbon Nanotubes. *Nano Lett.* **2007**, *7*, 398–402.
17. Crochet, J.; Clemens, M.; Hertel, T. Quantum Yield Heterogeneities of Aqueous Single-Wall Carbon Nanotube Suspensions. *J. Am. Chem. Soc.* **2007**, *129*, 8058–8059.
18. Tan, P. H.; Rozhin, A. G.; Hasan, T.; Hu, P.; Scardaci, V.; Milne, W. I.; Ferrari, A. C. Photoluminescence Spectroscopy of Carbon Nanotube Bundles: Evidence for Exciton Energy Transfer. *Phys. Rev. Lett.* **2007**, *99*, 137402/1−4.
19. Qian, H.; Georgi, C.; Anderson, N.; Green, A. A.; Hersam, M. C.; Novotny, L.; Hartschuh, A. Exciton Energy Tranfser in Pairs of Single-Walled Carbon Nanotubes. *Nano Lett.* **2008**, *8*, 1363–1367.
20. Kato, T.; Hatakeyama, R. Exciton Energy Tranfser-Assisted Photoluminescence Brightening from Freestanding Single-Walled Carbon Nanotube Bundles. *J. Am. Chem. Soc.* **2008**, *130*, 8101–8107.
21. Wong, C. Y.; Curutchet, C.; Tretiak, S.; Scholes, G. D. Ideal Dipole Approximation Fails To Predict Electronic Coupling and Energy Transfer between Semiconducting Single-Wall Carbon Nanotubes. *J. Chem. Phys.* **2009**, *130*, 081104/1−4.
22. Lefebvre, J.; Finnie, P. Photoluminescence and Förster Resonance Energy Transfer in Elemental Bundles of Single-Walled Carbon Nanotubes. *J. Phys. Chem. C* **2009**, *113*, 7536–7540.
23. Chen, F.; Ye, J.; Teo, M. Y.; Zhao, Y.; Tan, L. P.; Chen, Y.; Chan-Park, M. B.; Li, L.-J. Species-Dependent Energy Transfer of Surfactant-Dispersed Semiconducting Single-Walled Carbon Nanotubes. *J. Phys. Chem. C* **2009**, *113*, 20061–20065.
24. Lüer, L.; Crochet, J.; Hertel, T.; Cerullo, G.; Lanzani, G. Ultrafast Excitation Energy Transfer in Small Semiconducting Carbon Nanotube Aggregates. *ACS Nano* **2010**, *4*, 4265–4273.
25. Koyama, T.; Miyata, Y.; Asada, Y.; Shinohara, H.; Kataura, H.; Nakamura, A. Bright Luminescence and Exciton Energy Transfer in Polymer-Wrapped Single-Walled Carbon Nanotube Bundles. *J. Phys. Chem. Lett.* **2010**, *1*, 3243–3248.
26. Koyama, T.; Asaka, K.; Hikosaka, N.; Kishida, H.; Saito, Y.; Nakamura, A. Ultrafast Exciton Energy Transfer in Bundles of Single-Walled Carbon Nanotubes. *J. Phys. Chem. Lett.* **2011**, *2*, 127–132.
27. Jimenez, R.; Dikshit, S. N.; Bradforth, S. E.; Fleming, G. R. Electronic Excitation Tranfer in the LH2 Complex of *Rhodobacter sphaeroides*. *J. Phys. Chem.* **1996**, *100*, 6825–6834.
28. Pullerits, T.; Hess, S.; Herek, J. L.; Sundström, V. Temperature Dependence of Excitation Transfer in LH2 of *Rhodobacter sphaeroides*. *J. Phys. Chem. B* **1997**, *101*, 10560–10567.
29. Sumi, H. Theory on Rates of Excitation-Energy Transfer between Molecular Aggregates through Distributed Transition Dipoles with Application to the Antenna System in Bacterial Photosynthesis. *J. Phys. Chem. B* **1999**, *103*, 252–260.
30. Scholes, G. D. Long-Range Resonance Energy Transfer in Molecular Systems. *Annu. Rev. Phys. Chem.* **2003**, *54*, 57–87.
31. Beljonne, D.; Pourtois, G.; Silva, C.; Hennebicq, E.; Herz, L. M.; Friend, R. H.; Scholes, G. D.; Setayesh, S.; Müllen, K.; Brédas, J. L. Interchain *vs*. Intrachain Energy Transfer in Acceptor-Capped Conjugated Polymers. *Proc. Natl. Acad. Sci. U.S.A.* **2002**, *99*, 10982–10987.
32. Wong, K. F.; Bagchi, B.; Rossky, P. J. Distance and Orientation Dependence of Excitation Transfer Rates in Conjugated Systems: Beyond the Förster Theory. *J. Phys. Chem. A* **2004**, *108*, 5752–5763.
33. Swathi, R. S.; Sebastian, K. L. Excitation Energy Transfer from a Fluorophore to Single-Walled Carbon Nanotubes. *J. Chem. Phys.* **2010**, *132*, 104502/1–13.
34. Shafran, E.; Mangum, B. D.; Gerton, J. M. Energy Transfer from an Individual Quantum Dot to a Carbon Nanotube. *Nano Lett.* **2010**, *10*, 4049–4054.
35. Ando, T. Excitons in Carbon Nanotubes Revisited: Dependence on Diameter, Aharonov-Bohm Flux, and Strain. *J. Phys. Soc. Jpn.* **2004**, *73*, 3351–3363.
36. Wang, F.; Dukovic, G.; Brus, L. E.; Heinz, T. F. The Optical Resonances in Carbon Nanotubes Arise from Excitons. *Science* **2005**, *308*, 838–841.
37. Capaz, R. B.; Spataru, C. D.; Ismail-Beigi, S.; Louie, S. G. Diameter and Chirality Dependence of Exciton Properties in Carbon Nanotubes. *Phys. Rev. B* **2006**, *74*, 121401(R)/1−4.
38. Lüer, L; Hoseinkhani, S.; Polli, D.; Crochet., J.; Hertel, T.; Lanzani, G. Size and Mobility of Excitons in (6,5) Carbon Nanotubes. *Nat. Phys.* **2009**, *5*, 54–58.
39. Nakamura, A.; Tomikawa, T.; Watanabe, M.; Hamanaka, Y.; Saito; Ago, H. Non-linear Optical Response and Relaxation Dynamics in Double-Walled Carbon Nanotubes. *J. Lumin.* **2006**, *119−120*, 8–12.
40. Graham, M. W.; Chmeliov, J.; Ma, Y.-Z.; Shinohara, H.; Green, A. A.; Hersam, M. C.; Valkunas, L.; Fleming, G. R. Exciton Dynamics in Semiconducting Carbon Nanotubes. *J. Phys. Chem. B* **2011**, *115*, 5201–5211.
41. Miyata, Y.; Suzuki, M.; Fujihara, M.; Asada, Y.; Kitaura, R.; Shinohara, H. Solution-Phase Extraction of Ultrathin Inner Shells from Double-Wall Carbon Nanotubes. *ACS Nano* **2010**, *4*, 5807–5812.
42. O'Connell, M. J.; Bachilo, S. M.; Huffman, C. B.; Moore, V. C.; Strano, M. S.; Haroz, E. H.; Rialon, K. L.; Boul, P. J.; Noon, W. H.; Kittrell, C.; *et al.* Band Gap Fluorescence from Individual Single-Walled Carbon Nanotubes. *Science* **2002**, *297*, 593–596.
43. Weisman, R. B.; Bachilo, S. M. Dependence of Optical Transition Energies on Structure for Single-Walled Carbon Nanotubes in Aqueous Suspension: An Empirical Kataura Plot. *Nano Lett.* **2003**, *3*, 1235–1238.
44. Araujo, P. T.; Doorn, S. K.; Kilina, S.; Tretiak, S.; Einarsson, E.; Maruyama, S.; Chacham, H.; Pimenta, M. A.; Jorio, A. Third and Fourth Optical Transitions in Semiconducting Carbon Nanotubes. *Phys. Rev. Lett.* **2007**, *98*, 067401/1−4.
45. Lefebvre, J.; Fraser, J. M.; Homma, Y.; Finnie, P. Photoluminescence from Single-Walled Carbon Nanotubes: A Comparison between Suspended and Micelle-Encapsulated Nanotubes. *Appl. Phys. A: Mater. Sci. Process.* **2004**, *78*, 1107–1110.
46. Ohno, Y.; Iwasaki, S.; Murakami, Y.; Kishimoto, S.; Maruyama, S.; Mizutani, T. Chirality-Dependent Environmental Effects in Photoluminescence of Single-Walled Carbon Nanotubes. *Phys. Rev. B* **2006**, *73*, 235427/1−5.
47. Manzoni, C.; Gambetta, A.; Menna, E.; Meneghetti, M.; Lanzani, G.; Cerullo, G. Intersubband Exciton Relaxation Dynamics in Single-Walled Carbon Nanotubes. *Phys. Rev. Lett.* **2005**, *94*, 207401/1−4.
48. Ma, Y.-Z.; Valkunas, L.; Dexheimer, S. L.; Fleming, G. R. Ultrafast Exciton Dynamics in Semiconducting Single-Walled Carbon Nanotubes. *Mol. Phys.* **2006**, *104*, 1179–1189.
49. Förster, T. Zwischenmolekulare Energiewanderung und Fluoreszenz. *Ann. Phys.* **1948**, *2*, 55–75.
50. Dexter, D. L. A Theory of Sensitized Luminescence in Solids. *J. Chem. Phys.* **1953**, *21*, 836–850.
51. Reich, S.; Dworzak, M.; Hoffmann, A.; Thomsen, C.; Strano, M. S. Excited-State Carrier Lifetime in Single-Walled Carbon Nanotubes. *Phys. Rev. B* **2005**, *71*, 033402/1−4.
52. Hagen, A.; Steiner, M.; Raschke, M. B.; Lienau, C.; Hertel, T.; Qian, H.; Meixner, A. J.; Hartschuh, A. Exponential Decay Lifetimes of Excitons in Individual Single-Walled Carbon Nanotubes. *Phys. Rev. Lett.* **2005**, *95*, 197401/1−4.
53. Rubtsov, I. V.; Russo, R. M.; Albers, T.; Deria, P.; Luzzi, D. E.; Therien, M. J. Visible and Near-Infrared Excited-State Dynamics of Single-Walled Carbon Nanotubes. *Appl. Phys. A: Mater. Sci. Process.* **2004**, *79*, 1747–1751.
54. Wang, F.; Dukovic, G.; Knoesel, E.; Brus, L. E.; Heinz, T. F. Observation of Rapid Auger Recombination in Optically Excited Semiconducting Carbon Nanotubes. *Phys. Rev. B* **2004**, *70*, 241403(R)/1−4.
55. Ueda, A; Matsuda, K.; Tayagaki, T.; Kanemitsu, Y. Carrier Multiplication in Carbon Nanotubes Studied by Femtosecond Pump-Probe Spectroscopy. *Appl. Phys. Lett.* **2008**, *92*, 233105/1−3.